The Thesis Committee for Jacob Matthew Blacutt
Certifies that this is the approved version of the following Thesis:

Modulating the crosslinking of a hydrogel impacts cyclic-di-GMP signaling of *Pseudomonas aeruginosa*

APPROVED BY
SUPERVISING COMMITTEE:

Vernita Gordon, Supervisor

Lydia Contreras, Co-Supervisor

Modulating the crosslinking of a hydrogel impacts cyclic-di-GMP signaling of *Pseudomonas aeruginosa*

by

Jacob Matthew Blacutt

Thesis

Presented to the Faculty of the Graduate School of

The University of Texas at Austin

in Partial Fulfillment

of the Requirements

for the Degree of

Master of Arts

The University of Texas at Austin

May, 2020

Dedication

This thesis is dedicated to everyone that supported me in my time as a graduate student. A special dedication to my dog, Jake, and my friend, Alex, who both stayed with me through my most difficult times.

Acknowledgements

I'd like to thank Vernita Gordon for providing me with scientific guidance and introducing me to the world of physics research. Thank you to all the members of the Gordon lab and the Center for Nonlinear Dynamics for talking with me and helping me grow as a scientist and person.

Abstract

Modulating the crosslinking of a hydrogel impacts cyclic-di-GMP signaling of *Pseudomonas aeruginosa*

Jacob Matthew Blacutt, M.A

The University of Texas at Austin, 2020

Supervisor: Vernita Gordon

Co-Supervisor: Lydia Contreras

The growth of bacterial biofilms on medical devices is a persistent cause of device failure, necessitating removal, and infections that harm patients. Therefore, much effort has been expended on a variety of approaches to developing materials that resist biofilm development. However, to date the effects of varying the solid mechanics of the device material have not been tested. Biofilm development is initiated when bacteria attach to a surface, sense the surface, and begin the transition into the biofilm phenotype. For the common nosocomial pathogen *Pseudomonas aeruginosa* and many others, that transition is controlled by the second messenger cyclic-di-GMP. Here, we allow *P. aeruginosa* to attach to PEGDA gels and use a green fluorescent protein (GFP) reporter and laser-scanning confocal microscopy to measure the dynamics of the cyclic-di-GMP response in the first three hours after an initial hour-long attachment period. PEGDA gels are widely used in biomedical applications, in part because their mechanical properties are very tunable. We find that wild-type *P. aeruginosa* increase production of cyclic-di-GMP more

quickly when they attach to a stiffer PEGDA gel, with elastic modulus about 4000 kPa, than when they attach to a softer PEGDA gel, with elastic modulus about 50 kPa. Upon measuring the skewness and kurtosis of the per-cell GFP brightness distributions, we find that population's cyclic-di-GMP average is more heavily affected by a few strong responders, which upregulate cyclic-di-GMP production more quickly, on the softer gel than on the stiffer gel. Use of a mutant strain that does not make envelope protein PilY1, which has previously been suggested as a possible mechanosensor, shows that the WT's increased signaling speed on the stiffer surface is dependent on PilY1. Thus, the work presented here both contributes to the emerging field of bacterial mechanosensing and, speculatively, suggests that tuning the surface mechanics of medical devices might be a new approach to hindering biofilm development.

Table of Contents

List of Figures

1. Introduction

1.1 *Pseudomonas aeruginosa* background

1.1.1 *P. aeruginosa* as a pathogen

Pseudomonas aeruginosa is a species of Gram-negative bacteria that acts as an opportunistic pathogen in humans and other organisms[1,2]. Because it is an opportunistic pathogen, it mostly causes disease in individuals that have compromised immune systems. This pathogen is very prevalent in healthcare settings and is one of the major causes of nosocomial infections and resulting chronic infections[1]. In the United States alone, *P. aeruginosa* was the cause of an estimated 32,600 infections and 2,700 deaths in the year 2017, which resulted in medical care costs of around 727 million dollars[3]. One significant reason this pathogen infects so many individuals is that *P. aeruginosa* can form biofilms [1,2,4].

1.1.2 *P. aeruginosa* biofilms

P. aeruginosa is capable of forming robust biofilms on a multitude of materials [5]. These biofilms are bacterial communities existing in and surrounded by matrices made of multiple components including various polysaccharides, proteins, and environmental DNA[6]. Specifically, *P. aeruginosa* biofilms commonly contain the polysaccharides Pel, Psl, and alginate, which are present in various ratios depending on the strain of bacteria [6-7]. These polysaccharides can then crosslink with proteins such as CdrA to reinforce the biofilm matrix[8]. These materials together are referred to as extracellular polymeric

substances (EPS) and provide the bacterial communities inside tolerance to clearance from antibiotics and our immune system (Fig. 1.1) [8,10].

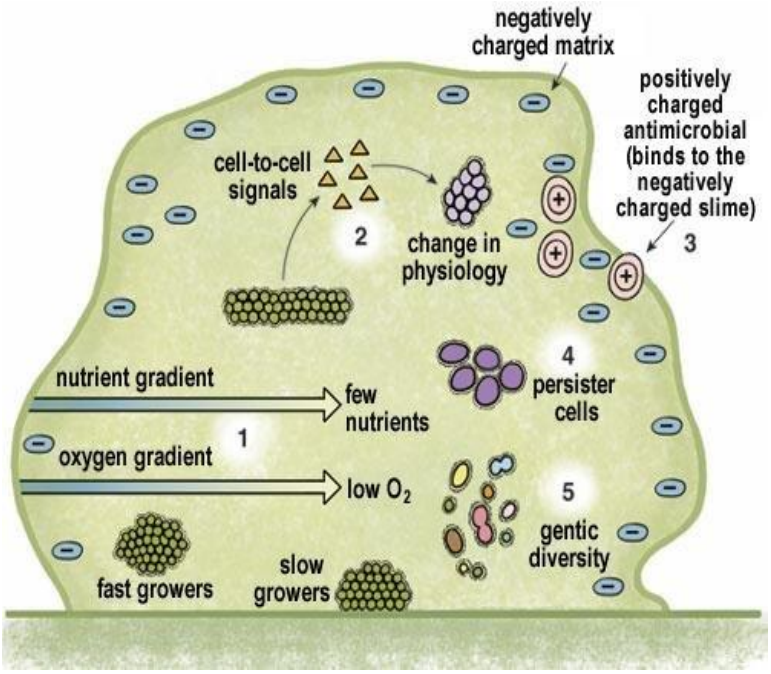

Fig 1.1 Structure of a bacterial biofilm

(1) Nutrient and oxygen gradients create populations of fast-growing cells in the biofilm periphery and slow-growing cells in the biofilm interior. (2) Quorum sensing within the biofilm further changes the physiology of cells inside. (3) Biofilms have negatively charged components that can bind and sequester positively charged antibiotics. (4) Biofilms contain diverse populations of cells including persister cells that are highly tolerant to antimicrobials. (5) Cells replicate and divide in biofilm matrices and create populations of cells with genetic diversity. Adopted from Dominguez-Benetton (2007) [9].

The biofilm provides increased tolerance to antibiotics through two main mechanisms. First, by reducing the oxygen availability and metabolic activity of bacterial cells on the interior of biofilms[11-12]. When cells are not metabolically active, they are less susceptible to antibiotics that target active metabolic processes such as translation[11-12]. The second mechanism providing increased antibiotic tolerance to biofilm cells is the binding and decreased availability of antibiotics in the biofilm matrix[13]. These two mechanisms together result in biofilms in which the cells on the interior of a biofilm can survive many treatments that would readily kill planktonic *P. aeruginosa.*

The biofilm protects bacterial cells from the immune system by resisting both our innate and adaptive immunity. *P. aeruginosa* biofilms can provide protection from the complement system by binding and sequestering complement proteins before they can bind to bacterial cells[14]. As a result, the complement system cannot be activated and no complement opsonization occurs. Bacterial cells within biofilms are also protected from phagocytosis by neutrophils by producing toxins that kill and lyse neutrophils[14]. Furthermore, neutrophils are mechanically limited in their phagocytosis and can possibly fail to pull out bacterial cells from a biofilm and engulf them[7].

1.1.3 *P. aeruginosa* biofilm formation

The biofilms are formed in several steps that start with planktonic bacteria that make physical contact with a surface[15-17]. After this initial contact they attach to that substrate reversibly and have a chance to detach and rejoin the planktonic population of cells[15]. However, cells that remain on a surface will become irreversibly attached and will

not easily leave the surface. In this stage many bacteria stay on a surface due to extracellular adhesins, which can bind strongly to certain surfaces[15]. Cells can then sense their attachment, and in *P. aeruginosa* and other species this results in an increase in intracellular cyclic-di-GMP (c-di-GMP) levels[18-20]. C-di-GMP is a second messenger that then signals cells to exit a planktonic lifestyle, and form microcolonies by secreting EPS[18]. These microcolonies start off as small monolayers of cells that quickly become 3D and then grow into larger colonies[20]. This growth is often referred to as biofilm maturation and can result in biofilms that are 1000 μM in diameter[21]. Cells can also be released from the biofilm at a later timepoint and once freed from the matrix can colonize new areas[15] (Fig. 1.2).

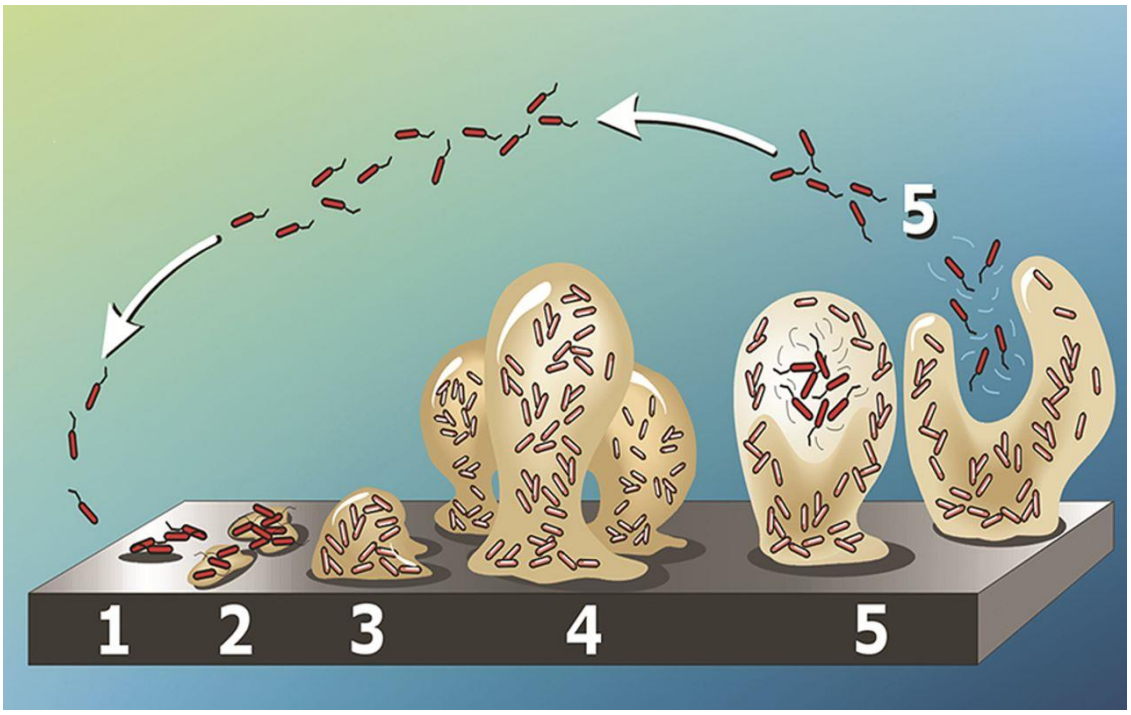

Fig. 1.2 Lifecycle of a biofilm
(1) Biofilm formation starts at reversible attachment, where cells attach to a surface, but can still easily detach and become planktonic. (2) This progresses to the point where cells irreversibly attach to a surface. (3) Bacterial cells begin to secrete EPS and form small communities called microcolonies. (4) Microcolonies mature into larger biofilms before (5) cells begin dispersing and leaving the mature biofilm. Adopted from Stoodley et al. (2002)[22]

1.2 *P. aeruginosa* and biomedical devices

1.2.1 Biofilm growth on biomedical devices

In most natural, non-laboratory settings, most bacteria live as part of biofilms, complex interacting communities often associated with surfaces [16,17,23]. Robust biofilms can form on a wide range of materials, are difficult to eliminate once formed, and resist both antibiotics and the immune system[24-25]. As a result, biofilms are a large and growing problem in the healthcare industry, estimated to be responsible for 80% of all microbial infections[26-28]. Biofilms have been observed to grow on many types of medical devices, from catheters to medical implants[29-32]. These complications are common; previous work has shown the infection rate of urinary catheters to be 26.6-35% and that of orthopedic implants to be 5-40% [26]. Given the difficulty of eliminating biofilms once they have formed, the most common approach to dealing with biofilms on medical devices is to remove the device, with consequent increased risk and suffering to the patient, and increased cost to the patient and the healthcare system at large [33]. A far better approach would be to develop medical devices that resist the development of biofilms in the first place. To this end, coatings have been developed that hinder biofilm growth by killing bacteria and by resisting the attachment of bacteria. The antimicrobial properties of surfaces are a result of either directly incorporating antibiotics into a coating or using a metal such as silver [32]. Antifouling coatings are made of materials varying from hydrogels to ceramic coatings that prevent attachment by affecting the hydrophilicity, topology, and interfacial energy of surfaces [34]. While these coatings are effective in

slowing down the colonization of bacterial biofilms, they have a limit in their effectiveness as they only target the attachment stage of biofilm development. A hitherto-unexplored alternative is to target the biological signaling that controls biofilm development.

1.2.2 *P. aeruginosa* attaching to biomedical devices

P. aeruginosa is responsible for many nosocomial infections in large part due to its ability to form biofilms on medical devices[5]. To form biofilms, planktonic *P. aeruginosa* attach to the surface of a medical device and increase their intracellular concentration of the second messenger cyclic-di-GMP (c-di-GMP) [35-37]. C-di-GMP controls the expression of many genes involved in biofilm formation; high intracellular levels of c-di-GMP are necessary for the shift from the non-biofilm, planktonic state to the biofilm state [18]. It is well-established that *P. aeruginosa* cells increase intracellular levels of c-di-GMP subsequent to attaching to rigid solid substrates such as glass, which has an elastic modulus of about 20 GPa [19,38,39]. While some work has explored the effect of varying substrate mechanics on the bacterial response to attachment, much work remains to be done to investigate how signaling is impacted by substrate mechanics[39-40].

We have recently shown that mechanical shear, which arises from surface attachment, can act as a cue for attachment and result in increased levels of c-di-GMP [19]. We showed this by modulating two environmental cues: the strength of bacterial attachment to the surface and the rate of fluid flow over bacteria attached to the surface. This suggests the possibility that bacteria could respond to other mechanical cues from

their environment, such as the mechanics of the substrate to which they attach. It is well known that cells from higher eukaryotes sense and respond to the mechanics of their substrate [41-43]. However, while a large body of research has studied mechanotransduction in higher eukaryotes, little is known about prokaryotic mechanosensing in any context, including that of biofilm formation[44-46]. Although the effects of surface topography and chemistry on bacterial attachment have been investigated [47-48], little work has been done to elucidate the effects of substrate mechanical properties on bacterial attachment and even less has been done to investigate how bacteria might use mechanosensing to respond to surface mechanics. In this work we investigate how substrate mechanics affect the response of the bacterial species *P. aeruginosa* to surface attachment by measuring changes in intracellular c-di-GMP signaling. In an extension of the technique we used previously[19], we use quantitative confocal microscopy to measure changes in the intensity of a green fluorescent protein (GFP) reporter for c-di-GMP, taking into account optical attenuation caused by the gel substrate.

1.2.3 PEGDA Hydrogels

One material of interest used in studies probing bacterial attachment and used in many biomedical applications is the poly(ethylene glycol) dimethacrylate (PEGDA) hydrogel [39,49-50]. These are gels composed of PEGDA molecules that are crosslinked into a mesh structure in the presence of UV light and a photoinitiator (Fig. 1.3). PEGDA hydrogels are biocompatible gels that have been used as 3D tissue engineered constructs [51-52] and matrices for controlled release of drugs[53-54]. These hydrogels can be synthesized

to have a range of porosities and stiffnesses by modulating the cross-linking density and concentration of the polymer; most applications have used gels with a compressive modulus of 2-70 kPa[55-56]. Importantly, earlier researchers have found that fewer bacteria attach to thick PEGDA hydrogels than to thin PEGDA hydrogels [40]. This makes PEGDA an ideal test material for a pilot study on the effect of substrate mechanics on bacterial mechanosensing and the resultant c-di-GMP signaling during attachment to a real-world biomedical material.

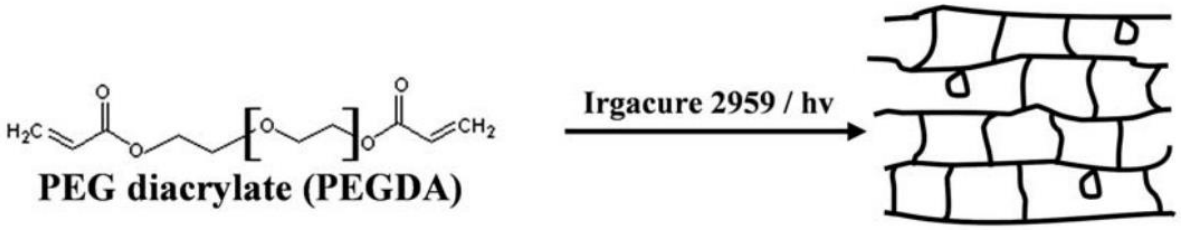

Fig 1.3 Structure of PEGDA

Structure of a standalone molecule (left) and crosslinked into a mesh (right). By changing the molecular weight of the PEGDA molecule you can increase the distance between crosslinks in the mesh and change the mechanics of the gel. Adopted from Browning et al. (2010) [56]

1.3 Mechanosensation

1.3.1 Eukaryotic mechanosensing

Mechanosensation is the transduction of mechanical stimulus to a biological signal. This process has been studied extensively in eukaryotes, and to a lesser degree in prokaryotic organisms[41-43]. In eukaryotic organisms mechanosensing starts when a mechanical stimulus changes the three-dimensional confirmation of cellular structures such as the plasma membrane, membrane-bound proteins, and the cytoskeletal network [41-43, 57]. The cells then sense these specific changes via one of multiple mechanosensors. Some of these sensors include integrin-based and cadherin-based adhesions, and force sensitive membrane proteins[57].

One system that has been particularly well studied is the focal adhesion based mechanosensory system in which mechanical stress changes the conformation of integrin, recruits more integrin to the plasma membrane, and regulates the interactions between proteins at the focal adhesion[57]. Changes in the focal adhesion structure then transduce the stimulus to the cytoskeleton and act as a signal to drive downstream signaling cascades that are regulated by effector proteins[57]. As a result, this promotes the expression of mechanosensitive genes, which then in turn regulate behaviors like cell proliferation and cell migration[57].

Force sensitive membrane proteins and specifically mechanosensitive ion channels are widely used in eukaryotic mechanosensing. These proteins function by changing shape in response to mechanical stimuli and either adopt an open or closed

conformation[58]. Proteins in the open conformation will allow the flow of ions across the plasma membrane, while proteins in the closed conformation will not allow the passage of ions[58]. Mechanosensitive ion channels can change conformation in response to membrane tension or force applied to the extracellular matrix[58]. Similar to mechanosensation via focal adhesions, these aid in regulation of cell volume, migration, and differentiation[58].

1.3.2 Prokaryotic mechanosensing

As previously mentioned, *P. aeruginosa* must attach to surface, sense their attachment, and increase their c-di-GMP concentration before they can begin forming a biofilm [18-20]. This is one example of prokaryotic mechanosensing that makes use of multiple mechanosensors with mechanisms that are to date still being elucidated. However, multiple putative mechanosensors have been studied in both *P. aeruginosa* and other bacterial species that are required to regulate surface associated behaviors [59]. These mechanosensors include flagella, type IV pili, and envelope proteins and they commonly regulate behaviors such as motility, EPS expression, and virulence[59].

Flagella, pili, and envelope proteins are all extracellular structures in bacteria that can transduce mechanical stimuli inwards to regulate gene expresion (Fig. 1.4). Flagella are extracellular structures that allow bacteria to swim in liquid environments and function by utilizing a proton gradient to spin the flagellar filament like a propeller [59]. When a bacterium encounters a vary viscous fluid or attaches to a surface the flagellum is no longer able to rotate freely. As a result, the flow of ions through the flagellar stators is

interrupted and can provide a clear cue of attachment to a bacterial cell. Another putative mechanosensor in bacteria are type IV pili. Type IV pili are filamentous extracellular structures that can extend by polymerizing more pilin proteins to the filament or retract by depolymerizing the filament [60]. When bacteria attach to a surface, attach a pilus, and then retract it they are creating tension on the filament. This tension acts as a signal for surface attachment that then transduces the signal inwards to regulate cellular behaviors such as virulence[59,61]. In *P. aeruginosa*, deletion of the major pilins of type IV pili or of the retraction motor abolishes surface associated behaviors [19,61]. Finally, envelope proteins have also been implicated as mechanosensors in prokaryotic cells. The best example of this is the *E. coli* CpxA–CpxR two-component system. This system is thought to function by sensing deformation in the cell membrane. It accomplishes this through sensing membrane stress with the outer membrane protein NlpE, which then activates the inner membrane protein CpxA[62]. CpxA then autophosphorylates itself before transmitting the phosphate group to the response regulator CpxR[61]. This regulator can then regulate the transcription of a number of target genes in *E. coli* [62].

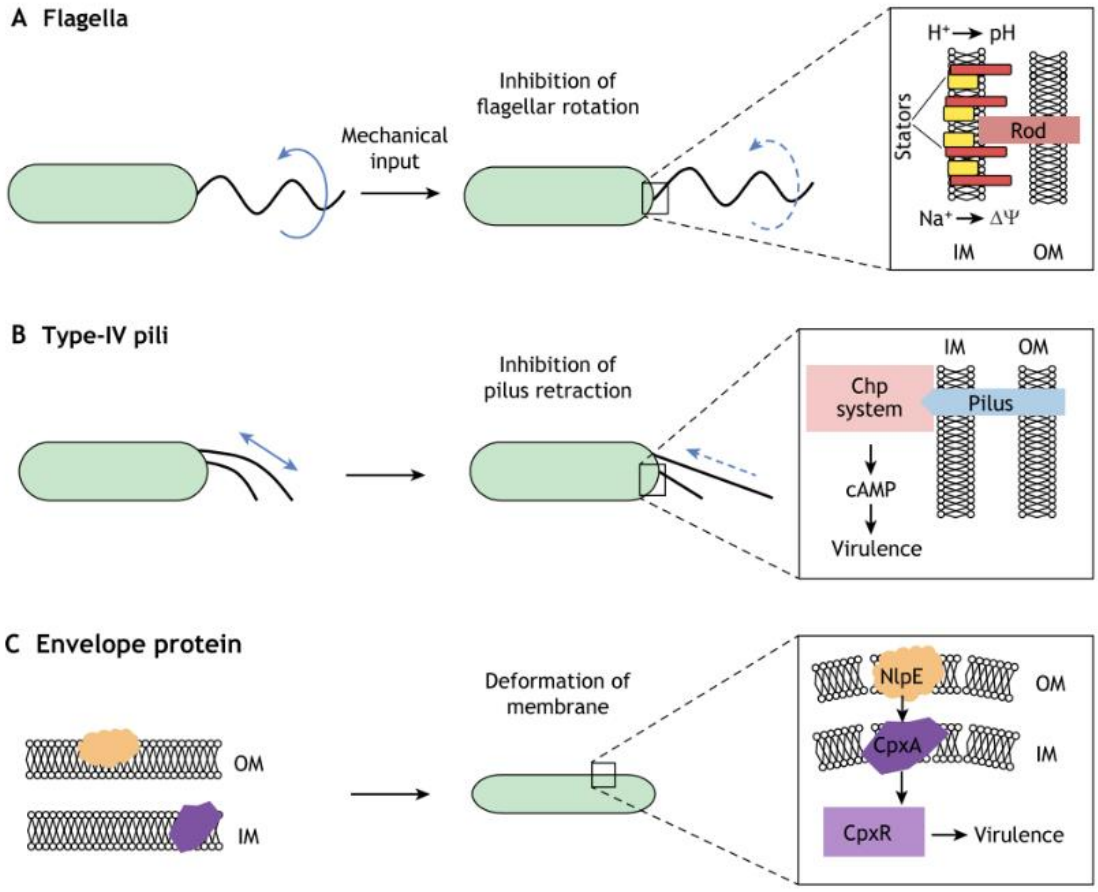

Fig 1.4 Bacterial mechanosensors and their proposed mechanisms
(A) Flagella. Inhibition of flagellum rotation can result from increased viscosity around the filament or contact with a surface. This can alter the flow of ions through the stators. (B) Type-IV pili. Inhibition of pilus retraction creates tension on the pilus and transduces the signal to the Chp system. (C) Envelope protein. Deformation of the membrane is transduced through NlpE and is transduced through the CpxA–CpxR two-component system. Adopted from Gordon et al. (2019)[59]

The genes regulated by mechanosensing allow cells to adapt to grow as a sessile organisms affixed to one location. In *P. aeruginosa* this often involves turning on virulence genes on attachment to a surface[61]. This aids *P. aeruginosa* during the establishment of chronic infections as the bacteria can form biofilms where the cells inside are creating toxins to kill immune cells [61]. In *P. aeruginosa* and other bacteria attachment is also used as a cue to decrease the expression of genes involved in motility[59]. Understandably, bacteria must reduce their expression of genes involved in swimming motility using flagella and twitching motility using type IV pili if they wish to enter a lifestyle in which they are nonmotile. Finally, as mentioned before, mechanosensing regulates the production of EPS components that make up the biofilm[18,59]. In *P. aeruginosa* and other species of bacteria this is accomplished by the increase in c-di-GMP upon attachment which then aids in the downstream regulation of EPS production genes[18].

1.4 Rationale for thesis

Here we show that *P. aeruginosa* cells have a faster, stronger c-di-GMP signaling response subsequent to attachment on a stiff PEGDA gel, with elastic modulus 4000 kPa, than they do subsequent to attachment on a soft PEGDA gel, with elastic modulus 50 kPa. Our experiments lasted for the first 180 minutes after an initial surface attachment period of 60 minutes. We measured the fluorescence of our cells every 30 minutes and at every timepoint the difference in cyclic-di-GMP signaling on the two gel types was statistically significant. Furthermore, we show that the differentiation between surfaces

is affected by the presence of PilY1, as cells lacking PilY1 have statistically-significant differences from wild-type (WT) cells in c-di-GMP signaling dynamics following surface attachment. Specifically, we see that WT cells respond faster and with less heterogeneity when attached to gels in comparison to cells lacking Pily1. With this pilot study we exhibit the importance of substrate mechanics for biomedical devices and demonstrate that, irrespective of surface chemistry, the signaling necessary for biofilm formation can be impacted solely through surface mechanics. Furthermore, we demonstrate that the difference in signaling between surfaces is impacted by a bacterial envelope protein, Pily1. Here we provide a first look at the interplay between bacterial mechanosensors, surface mechanics, and signaling dynamics. This has the potential to inform the future design of medical devices such that their surface chemistry and mechanics work together to prevent the formation of biofilms.

2. Materials and Methods

2.1 Bacteria Strains

We used wild-type (WT) *P. aeruginosa* strain PAO1 and the transposon mutant Δ*pilY1* PAO1 in our experiments [63]. The Δ*pilY1* strain does not make the envelope protein PilY1. To study intracellular c-di-GMP levels, both strains were transformed with the reporter plasmid pCdrA::*gfp*. In this plasmid the expression of green fluorescent protein (GFP) is under the control of the promoter for the gene *cdrA.* This gene is transcriptionally controlled by c-di-GMP and therefore increased c-di-GMP results in an increase in fluorescence intensity [64]. Both WT and Δ*pilY1* PAO1 were also transformed

with the plasmid pMH487 instead of the reporter plasmid. The plasmid pMH487 contains a promotorless GFP gene and thereby provides a control measurement of background metabolic activity. Bacteria were grown on LB agar (Fisher BioReagents™ LB Agar, Miller) and in LB media supplemented with Gentamicin (Gentamicin Sulfate, Sigma-Aldrich) at a concentration at 60 µg/mL for the purpose of plasmid selection.

2.2 Bacterial Growth and Media

We grew all bacterial strains as we previously described [19]. In brief, we first streaked frozen stocks onto plates made of LB agar supplemented with Gentamicin at 60 µg/mL (LB agar is made using 5 g of yeast extract, 10 g of tryptone, 10 g of sodium chloride, and 15 g of agar per L of deionized water). After streaking, the plates were incubated at 37°C for 20 hours. Subsequently, we picked a single colony and used it to inoculate 5mL of LB media supplemented with Gentamicin at 60 µg/mL. The resulting culture was then shaken in an orbital shaker (Labnet Orbit 1000) operating at 235 rotations per minute for a period of 16-18 hours. We diluted 40µL of the overnight culture into 5mL of fresh LB media and these bacteria were then used in our experiments.

2.3 PEGDA Polymer Synthesis

PEGDA was synthesized as previously described [56,65]. In short, acryloyl chloride was added in a dropwise fashion to a solution of polyethylene glycol (PEG) and triethylamine in anhydrous dichloromethane (DCM) under nitrogen. The mixture contained PEG, acryloyl chloride, and triethylamine in a molar ratio of 1:2:4. This

mixture was then stirred for 24 hours at room temperature. We washed the solution with eight molar equivalents of 2M potassium bicarbonate and subsequently dried with anhydrous sodium sulfate. Finally, the product was precipitated in cold diethyl ether, filtered, and dried under a vacuum.

2.4 PEGDA Hydrogel Fabrication

PEGDA gels were fabricated as previously described [56]. In short, PEGDA powder of different molecular weights (2 or 10 kDa) was mixed with deionized water at different concentrations to make a precursor solution. These solutions were vortexed until dissolved and photoinitiator (Sigma Irgacure 2959) at a concentration of 1mg per 10µL 70% ethanol was added at 1% of the volume of the precursor. 4 µl of this solution was then pipetted into casting molds consisting of an imaging spacer liner (Grace Bio-Labs SecureSeal™ Imaging Spacers) placed onto a coverslip and sealed against a glass plate. We then exposed the PEGDA solution to long wave UV light (Ultraviolet Products High Performance UV Transilluminator,365 nm, 1 mW/cm^2) for a duration of 12 minutes. After curing we soaked the gels for 20 hours in Dulbecco's Phosphate Buffered Saline (Sigma) before imaging.

2.5 Mechanical Characterization of PEGDA Hydrogels

To characterize the mechanical properties of hydrogels used in our experiments, we performed compression tests. In these tests we first punched out six 8-mm discs from

a single gel for each of our formulations for testing. We tested these samples using a dynamic mechanical analyzer (RSAIII, TA Instruments) equipped with a parallel-plate compression clamp. In our characterization we performed a dynamic strain sweep to determine the linear viscoelastic range for our formulations. Subsequently, a strain in the upper portion of the linear viscoelastic range was used in a constant-strain frequency sweep. To determine the final compressive the frequency sweep was conducted between 0.79 and 79 Hz and the storage modulus was recorded at 1.25 Hz for each gel [56]. Finally, the moduli of the multiple discs were averaged to obtain the average compressive modulus for each PEGDA hydrogel formulation.

2.6 Laser-Scanning Confocal Fluorescence Microscopy

For all experiments, we used an Olympus FV1000 motorized inverted IX81 microscope suite, with instrument computer running FV10-ASW, version 4.2b, software, to image attached bacteria using laser-scanning confocal microscopy. To prepare the bacteria we first diluted 40 µL of an overnight culture into 5 mL of fresh LB media containing gentamicin. We then placed an imaging spacer (Grace Bio-Labs SecureSeal™ Imaging Spacers) on both the microscope slide and coverslip around the PEGDA gel. 25 µL of the bacterial dilution was inoculated onto the PEGDA gel substrate on a glass coverslip, sealed to a microscope slide, and bacteria were allowed to adhere to the gel for an hour prior to imaging. The slide was then placed on the microscope stage and imaged with a 60x oil-immersion objective, a 488-nm laser with a 405/488 excitation filter, and an emission filter of 505/605. For each day's worth of experiments, 10-15 sites were

imaged every 30 minutes for a total of 3 hours. This process was repeated on three different days for each condition. To image each site a confocal Z-stack was taken with a depth of 6 μm and an interval size of 750 nm.

2.7 Image processing and analysis

We used the Fiji distribution of ImageJ software (version 1.52) for image processing [66]. Each z-stack was projected to create both a maximum intensity projection and an average intensity projection on the x-y plane. The locations of single cells were determined on the average intensity projections to exclude cells that were not attached and only present in a single frame of the z-stack. The mean fluorescence intensities of individual cells were then determined using the maximum intensity projections. These data were then and analyzed in R (Ver. 3.6.1) to obtain our plots and statistical significance values.

2.8 Accounting for fluorescence attenuation

To account for the attenuation of exciting and emitted light passing through different gels, we used green fluorescent beads (Dragon Green, Bangs Laboratories, Inc.) that are similar in both their excitation and emission spectra to GFP-expressing bacteria, thus acting as a model for how the GFP excitation and emission light is affected by passing through the gel. We measured the brightness of these beads using the same laser, but we used a different intensity, photomultiplier, and image acquisition setting than we used for measuring bacterial brightnesses.

3. Results

3.1 Hydrogel mechanics

To probe how bacteria respond to substrate stiffness, we made use of highly tunable hydrogels composed of poly(ethylene glycol) diacrylate (PEGDA) that vary in stiffness from 4000 kPa to 50 kPa . The mechanics of these hydrogels were tuned in two ways; by changing the molecular weight of the PEGDA used and by altering the concentration of PEGDA in the precursor solution [56]. Specifically, we allowed *P. aeruginosa* to attach either to a stiff hydrogel composed of PEGDA with an average mass of 2k Da, dissolved at a concentration of 50% w/v in the precursor solution, or to a soft hydrogel composed of PEGDA with an average mass of 10k Da, dissolved at a concentration of 10% w/v in the precursor solution. We determined the mechanics of these two types of gel by measuring their compressive moduli using a dynamic mechanical analyzer.

We found that when the hydrogels were tested, they had significantly different compressive moduli. Specifically, the PEGDA hydrogel made of 2k Da PEG had a compressive modulus of around 40000 kPa, while the PEGDA hydrogel made of 10k Da had a compressive modulus around 50 kPa (Fig. 3.1). While the hydrogels are chemically very similar this mechanical characterization shows that these gels are mechanically very distinct.

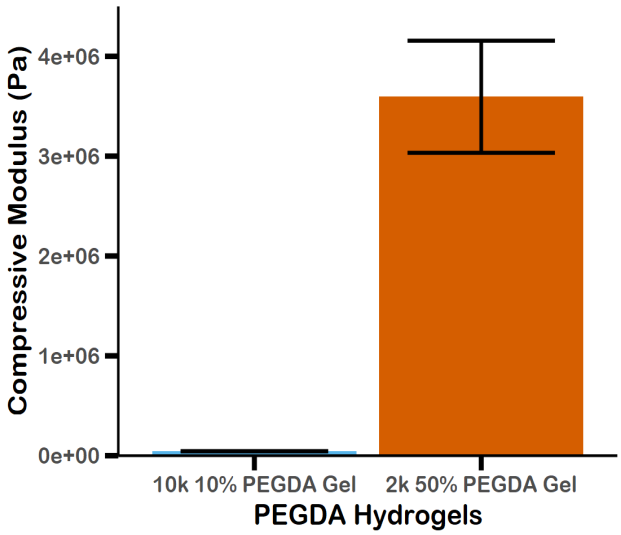

Fig. 3.1 Compressive modulus of PEGDA gels.

Shown are the compressive moduli of our two PEGDA hydrogel formulations determined using a dynamic mechanical analyzer. Error bars represent the standard error of our measurements. We found that our hydrogels were very mechanically different and that our stiff hydrogel is around 4000 kPa and our soft gel is around 50 kPa.

3.2 Accounting for the effects of optical attenuation and changes in bacterial metabolism

By using *P. aeruginosa* cells containing the plasmid pCdrA::gfp, which is a verified reporter for c-di-GMP [64], we were able to monitor the dynamics of intracellular c-di-GMP concentrations over the first three hours after bacteria attached to a gel substrate for a period of one hour. Data was collected by imaging cells with a laser scanning confocal microscope at 30 minute intervals (Fig. 3.2 A and B).

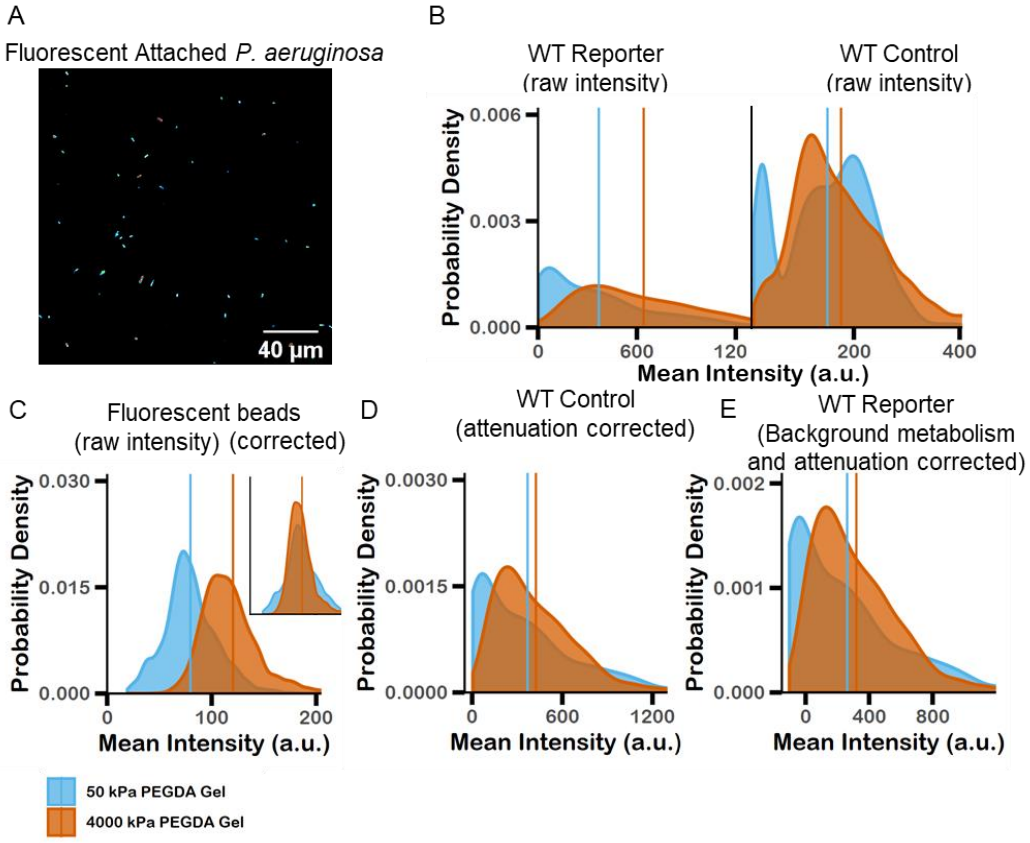

Fig. 3.2 Fluorescence calibration of WT reporter PA01

(A) Example fluorescence image analyzed to generate probability density distributions. (B) Uncalibrated fluorescence intensity of individual PA01 WT pCdrA::gfp cells (left) and PA01 WT pMH487 cells (right) on both the 10k PEGDA gel (soft) and 2k PEGDA gel (stiff). (C) First step in calibrating fluorescence intensities of individual cells. Briefly, fluorescent beads were imaged on both gels and then an attenuation factor was determined such that when it was applied to the fluorescence intensities of all beads on the stiff gel the mean values in both conditions were equal (inset). (D) Intensity distributions of control vector strain (PA01 pMH487) with the bead calibration applied. In the control plasmid the average fluorescence was higher on the 50 kPa (soft) PEGDA gel. (E) Fluorescence intensity distributions of PA01 pCdrA::gfp cells with calibration from the fluorescent beads attenuation factor and subtracted mean intensity values from the control vector. The average fluorescence was higher on the 4000 kPa (stiff) PEGDA gel.

Different gel substrates could cause different attenuation both of the light used for fluorescence excitation and of the fluorescently-emitted GFP light. Therefore, we measured the intensities of fluorescent beads, on the two types of gel substrates, that have both excitation and emission spectra similar to those of GFP-expressing bacteria. Thus, the beads acted as a model for how the GFP excitation and emission light was affected by passing through the gel. We found that the beads are brighter when imaged on the 2k 50% PEGDA gels than when imaged on the 10k 10% PEGDA gel. We then calculated an attenuation factor of 0.662 that, when applied to all of the fluorescence intensity values of the beads on the 2k 50% PEGDA gel, collapses the average fluorescence intensities on both the 10k PEGDA gel and the 2k PEGDA gel to the value 79.6 a.u. (Fig. 3.2 C). This attenuation factor was applied to raw fluorescence data for both reporter and control strains of *P. aeruginosa*. Control strains contain the promoter-less GFP plasmid pMH487 (Fig. 3.2 D).

To control for differences in the baseline metabolism of bacteria across different substrates, we then subtracted the attenuation-corrected average fluorescence intensity of control bacteria at each timepoint from the measured intensities of reporter bacteria on the same type of gel. This removes fluorescence that is a result of the normal metabolism of these cells and leaves only the fluorescence that arose as a result of intracellular c-di-GMP levels (Fig. 3.2 E).

3.3 Substrates of different stiffnesses are associated with different c-di-GMP signaling patterns

We use the Kolmogorov–Smirnov (KS) test for comparing two distributions to compare brightness distributions of populations of bacterial cells on soft (50 kPa) and stiff (4000 kPa) hydrogels at the same timepoint after attachment (Fig. 3.3 A) and to compare brightness distributions on the same type of gel at different timepoints (Fig. 3.3 B) [67]. Using attenuation and metabolism corrected brightness distributions, we find that populations on stiff and on soft PEGDA substrates have statistically significant differences throughout the three hours we measured after attachment to the substrate (Fig. 3.3 A). Populations on both types of gels change their brightness distributions to a statistically-significant level during the timescale of observation (Fig. 3.3 B), but the increase in fluorescence is greater over the period from 60 to 120 minutes in bacteria attached to the stiff substrate in comparison to bacteria attached to the soft substrate (Fig. 3.3 C).

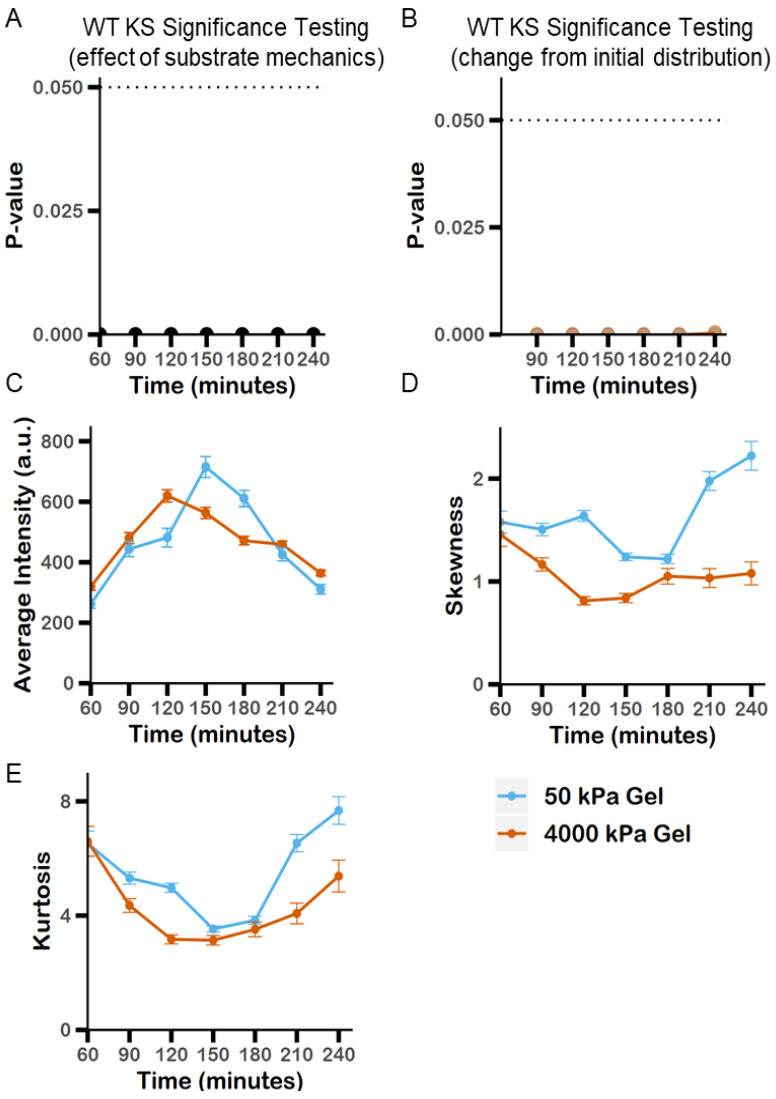

Fig. 3.3 Analysis of WT PA01 fluorescence distributions

Comparison between distributions of fluorescence intensities of PA01 WT cells on the 4000 kPa (stiff) PEGDA gel and the 50 kPa (soft) PEGDA gel. P-values are obtained from the Kolmogorov–Smirnov test. (A) The fluorescence intensity was significantly different between both PEGDA gels for every timepoint. (B) Comparison of distributions of fluorescence intensities from time 60 to all subsequent time points for both the stiff and soft gel. P-values are obtained from the Kolmogorov–Smirnov test. For the bacteria on the stiff gel, the difference from time 60 was significant at all time points. Additionally, the bacteria on the soft gel experienced significant differences from time 60 at all subsequent times. (C) Average fluorescence intensities of all single cells attached to both the soft and stiff gel for three hours. We see that the bacteria attached to the stiff gel reach their peak fluorescence earlier at 120 minutes in comparison to 150 minutes for bacteria attached to the soft gel. (D) Skewness of fluorescence intensity distributions at every time point. In both conditions we see distributions that are skewed right. (E) Kurtosis of fluorescence intensity distributions at every time point. The kurtosis value is higher on the soft gel than on the stiff gel. This signifies a higher presence of extreme data points or outliers.

This is in agreement with our finding that the average fluorescence intensity is greater on the 4000 kPa hydrogel in our early timepoints, 60 minutes through 120 minutes post attachment, and that the change in average fluorescence intensity from 90 minutes to 120 minutes after attachment is also greater on the 4000 kPa hydrogel (Fig. 3.3 C). However, at 150 minutes, bacterial populations on the softer, 50 kPa hydrogel reached higher levels of fluorescence intensity corresponding to a higher level of c-di-GMP (Fig. 3.3 C). From these results we note that substrate mechanics may impact the timescale of surface sensing and the total c-di-GMP "dose" experienced by bacteria in early times after attachment.

Other researchers have previously shown that *P. aeruginosa* populations are heterogeneous in their response to surface attachment [68]. In short, it was found that upon attachment of *P. aeruginosa* to a surface, one subpopulation of cells would robustly increase its intracellular c-di-GMP concentration and begin biofilm formation, while another subpopulation would retain low c-di-GMP levels and engage in more surface motility. To examine how a heterogeneous response might interplay with substrate stiffness, we measured the skewness and kurtosis of all attenuation and metabolism corrected brightness distributions - skewness to determine asymmetry and kurtosis to determine the preponderance of outliers [69].

We see that the skewness and kurtosis are higher for populations attached to the softer gel for all timepoints (Fig. 3.3 D and E). This shows that the populations of cells attached to the softer substrates contain more outliers and therefore a more distinct

subpopulation of “strong responders”. In contrast, bacteria attached to the stiff gel have less outliers and have a population with a greater proportion of cells that are robustly responding to attachment to increase c-di-GMP concentration. Thus, not only is c-di-GMP higher in cells attached to stiffer substrates, but a greater proportion of the population is able to respond to the mechanical cues generated upon attachment to a surface. These results suggest that substrate mechanics may impact the development of heterogeneity in populations of surface-attached bacteria.

3.4 Loss of the membrane protein PilY1 impacts the timescale of surface sensing

We and others have found that the envelope protein PilY1 is required for *P. aeruginosa* to increase c-di-GMP levels following attachment to a rigid surface and strongly impacts other surface-associated behaviors [70-71]. We have previously suggested that PilY1 could act as a mechanosensor to transduce the mechanical signal(s) induced by surface attachment[19]. Here we use *Δpily1*, which does not make PilY1, to probe the importance of this envelope protein for discriminating between two types of hydrogels with different stiffnesses by responding to attachment with different levels of c-di-GMP (Fig. 3.4), using the same experimental and analytical procedure described above for WT.

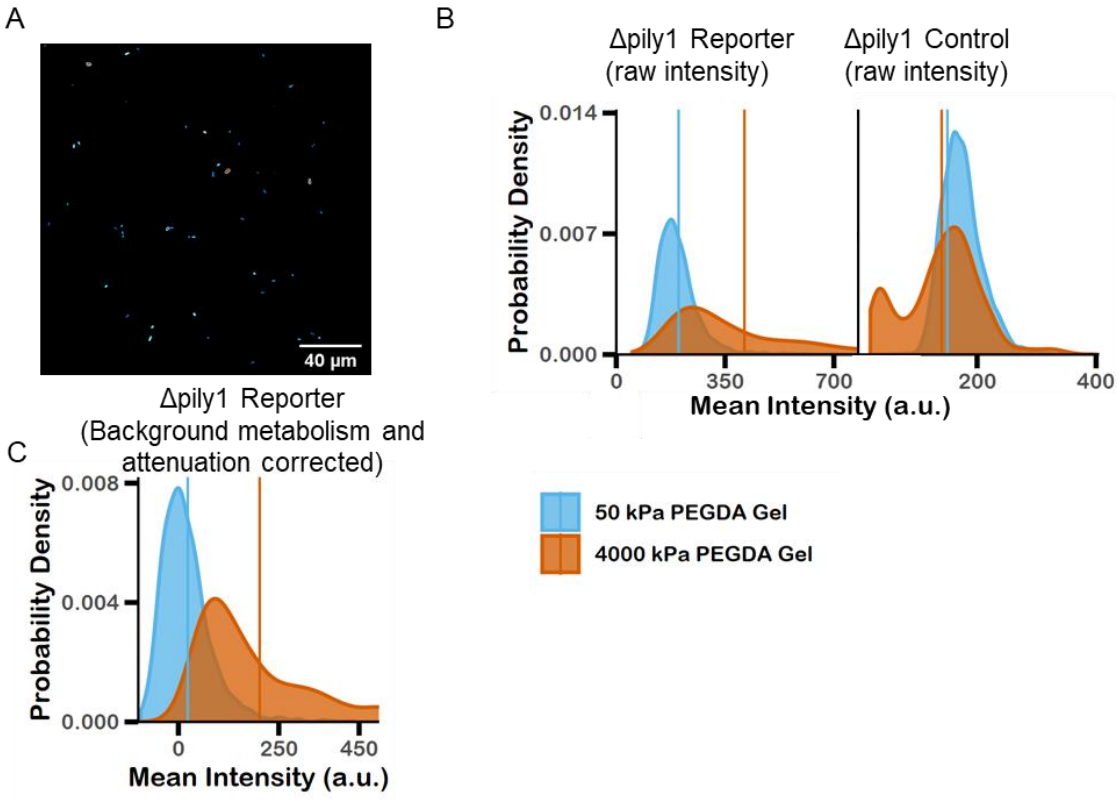

Fig. 3.4 Fluorescence calibration of Δpily1 reporter PA01
(A) Example image of attached Δpily1 cells. (B) Uncalibrated fluorescence intensity of individual PA01 Δpily1 pCdrA::gfp cells (left) and PA01 Δpily1 pMH487 cells (right) on both the 10k PEGDA gel (soft) and 2k PEGDA gel (stiff). (C) Fluorescence intensity distributions of PA01 Δpily1 pCdrA::gfp cells with calibration from the fluorescent beads attenuation factor and subtracted mean intensity values from the control vector. The average fluorescence was higher on the 4000 kPa (stiff) PEGDA gel.

As for the WT cells, the fluorescence intensity distributions of populations of reporter *Δpily1* bacteria on the two gel types are different at statistically significant levels at every timepoint (Fig. 3.5 A). However, in contrast to WT (Fig. 3.3 B), the fluorescence intensity distributions of *Δpily1* populations are not different from their initial distribution at every subsequent timepoint, to a statistically significant degree (Fig. 3.5 B). Instead we see that bacteria attached to the stiff gel return to their fluorescence intensity observed at 60 minutes at 240 minutes (Fig. 3.5 B). Similar to our observations of WT cells we find that the average fluorescence intensity of reporter *Δpily1* bacteria on the stiffer gel is higher at statistically significant levels at every timepoint in comparison to the fluorescence observed on the softer gel (Fig. 3.5 C). Interestingly, while bacteria on the stiff gel are more fluorescent regardless of the presence of Pily1, the timescale of signaling is different between WT and *Δpily1* cells. WT cells increase their fluorescence on the stiff gel over the initial 60 minutes of observation and peak at 120 minutes (Fig. 3.3 C). In contrast *Δpily1* cells on the stiff gel do not increase their fluorescence in the initial 30 minutes of observation and obtain their peak fluorescence later at 150 minutes (Fig. 3.5 C).

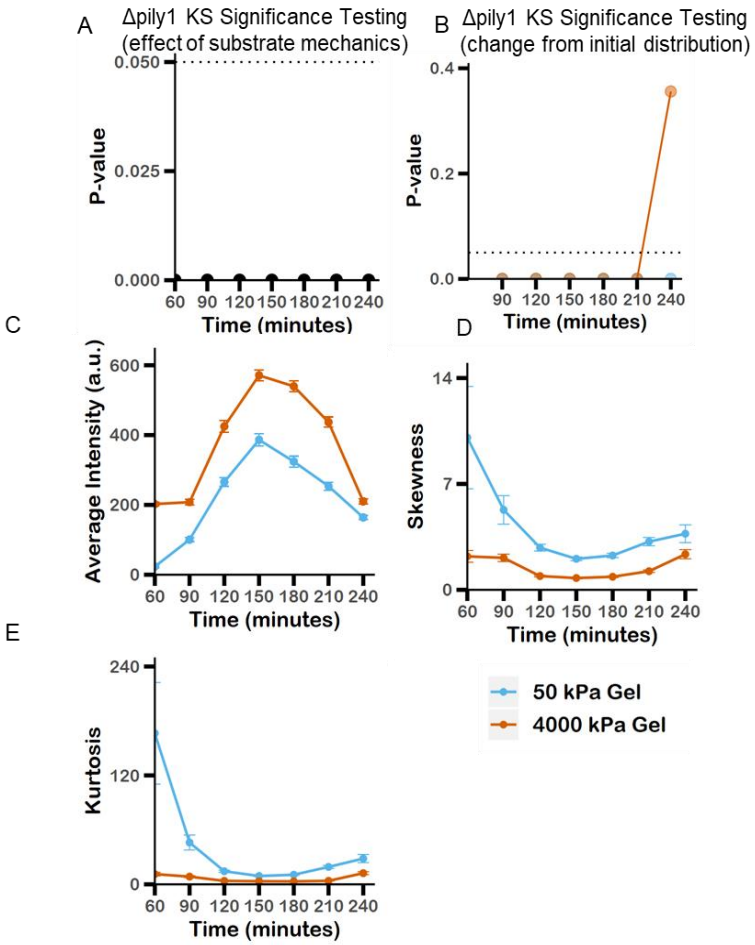

Fig. 3.5 Analysis of Δpily1 PA01 fluorescence distributions
(A) Comparison between distributions of fluorescence intensities of PA01 Δpily1 cells on the 4000 kPa (stiff) PEGDA gel and the 50 kPa (soft) PEGDA gel. P-values are obtained from the Kolmogorov–Smirnov test. The fluorescence intensity was significantly different between both PEGDA gels for every timepoint. (B) Comparison of distributions of fluorescence intensities from time 60 to all subsequent time points for both the stiff and soft gel. P-values are obtained from the Kolmogorov–Smirnov test. For bacteria attached to both gels we see a significant difference at every timepoint, except for bacteria attached to the stiff gel where they returned to their original measured fluorescence at 240 minutes. (C) Average fluorescence intensities of all single cells attached to both the soft and stiff gel for three hours. (D) Skewness of fluorescence intensity distributions at every time point. In both conditions we see distributions that are skewed right and that the distributions from the soft gel condition are more skewed to the right. (E) Kurtosis of fluorescence intensity distributions at every time point. The kurtosis value is higher for the distributions of bacteria attached to soft gels at every timepoint. This signifies a higher presence of extreme data points or outliers. In both conditions the kurtosis values are highest at the end timepoints.

3.5 Loss of the membrane protein PilY1 increases heterogeneity in c-di-GMP signaling on both soft and stiff substrates

In *Δpily1* populations the kurtosis and skewness of the brightness distributions is highest in cells attached to the soft hydrogel and highest in our initial and final observations on both the soft and stiff gels (Fig. 3.5 D and E). Both kurtosis and skewness are higher for *Δpily1* populations at both initial and final timepoints (Fig. 3.5 D and E) than for WT at the same times (Fig. 3.3 D and E). These data demonstrate that as populations of *Δpily1* bacteria attach to surfaces their changes in c-di-GMP levels are more heavily impacted by outliers consisting of "strong responders".

This difference combined with the finding that WT cells reach their peak c-di-GMP concentration faster on stiff gels than *Δpily1* cells suggest that Pily1 is important in the regulating the response to surface attachment in *P. aeruginosa*. Specifically, without Pily1 response to our stiff surfaces requires more time and creates populations with more heterogenous responses on both gels. This corroborates our previous observations and the observations of others that Pily1 is used to regulate the response of *P. aeruginosa* to different surfaces.

4. Discussion

In our data we saw that the c-di-GMP production in wild-type cells responded differently during attachment to hydrogels of different stiffnesses. We also saw a difference in c-di-GMP production in Δpily1 cells when attached to hydrogels with differing mechanics, but on a different timescale. These observations suggest that the

protein PilY1 is used to regulate a response to attachment but is not the only mechanism that exists that allows *P. aeruginosa* to distinguish between different surfaces. When we look at the dynamics of c-di-GMP production in these two populations we notice stark differences. Particularly, when we look at the first hour of attachment, we see that wild-type cells produce c-di-GMP at a faster timescale when on stiff gels, whereas Δpily1 bacteria respond at the same timescale independent of which hydrogel they attached to. This suggests that while Δpily1 is used for mechanosensing, it alone is not the sole contributor to the *P. aeruginosa* surface response.

Work by others has shown that show deletion of PilY1 was not enough to abolish all responses to mechanical stimuli [68,72-73]. Previous work has also suggested that type IV pili [19,38] and flagella [74-75] also serve a mechanosensory role. In line with those findings, it is possible that our *Δpily1* bacteria produce other extracellular mechanosensors that still allow *P. aeruginosa* to differentiate between different substrates even if the dynamics of the response are different. However, it is possible that the *Δpily1* bacterial cells are differentiating between our two substrates not based on mechanical cues, but on another feature of our substrates.

We speculate the mesh size of our two substrates could be affecting our measurements of surface response in addition to their stiffnesses. The mesh size of our gels affects the diffusion of nutrients through those materials and the availability of nutrients could be a factor in generating the surface response of attached bacteria. Specifically, we expect that the mesh size in our soft gel will be relatively large when

compared to our stiff gel and allow for attached bacteria to grow an environment with greater nutrient availability. We make this prediction because the PEG used in our stiff gel has a molecular weight of 2000 and is present at a 50% w/v ratio, while the molecular weight of the PEG used in our soft gel has a molecular weight of 10000 and is present at a 10% w/v ratio. These together clearly suggest that the distance between the crosslinks in our soft gel should be longer than that distance in our stiff gels and result in a larger mesh size and increased diffusion.

5. Conclusion and future perspectives

We have found that *P. aeruginosa* WT PAO1 responds with c-di-GMP signaling more quickly, and with more strong responders, when they attach to a stiff PEGDA gel surface than when they attach to a soft PEGDA gel surface. C-di-GMP is a second messenger that controls the transition from a planktonic to a biofilm state, so this may result in different dynamics of biofilm development on gels with different mechanics. In future work we will study how these changes in c-di-GMP signaling impact mature biofilm architecture. This kind of study would advance our understanding of bacterial signaling and how that leads signaling to biofilm formation. Rather than looking only at the concentrations of messenger in a cell, we will look at the changing concentration on the minute time scale and correlate these to biofilm structure. This is important as we have seen in our data that *P. aeruginosa* does not increase c-di-GMP at the same rate when attached to different surfaces and that the increase in c-di-GMP associated with surface association does not last for the entire duration of attachment. This would allow

us to possibly steer bacteria into forming biofilms with weak architectures that are highly susceptible to clearance via our immune system or through antimicrobial treatments.

PEGDA gels are already used in biomedical applications and one of their appealing properties is their mechanical tenability. Bacterial biofilms are a significant problem in healthcare contexts. If future work shows that different c-di-GMP signaling responses can be controlled by adjusting PEGDA gel moduli and that these result in impaired biofilm development, this could be a promising new category of approaches to making medical devices resistant to biofilm development. In future work it would be useful to study the outcomes of medical devices coated in PEGDA gels with various mechanical properties. It is our hope that PEGDA could be used as a coating to reduce the rate of biomedical device failure and alleviate the associated burden of device failure on both patients and our healthcare system.

Finally, we saw that the discriminatory response to PEGDA gels of different elasticity, by different levels and timescales of c-di-GMP upregulation, is altered when the envelope protein PilY1 is lost. This suggests a role for this protein in the preferential rapid response to a stiffer surface. This is plausible given the previous work showing that Pily1 contains a domain homologous to the von Willenbrand factor, a domain present in eukaryotic mechanosensing proteins[76], and the work showing that surface associated behaviors require Pily1. This advances our understanding of bacterial mechanosensing as it further supports previous studies that implicate Pily1 as a mechanosensor. Additionally, by studying how the dynamics of c-di-GMP signaling are impacted and not just the

overall concentrations we will obtain a better understanding of what mechanical cues are sensed by Pily1. In further studies, we will study how the loss of other mechanosensors, namely flagella and type IV pili, also impact the dynamics of c-di-GMP signaling on attachment to various surfaces. After such studies we will have a better understanding regarding the structures bacteria use to mechanosense and exactly what mechanical stimuli they require to function.

References

1. Moradali, M. F., Ghods, S., & Rehm, B. H. A. (2017). Pseudomonas aeruginosa lifestyle: A paradigm for adaptation, survival, and persistence. *Frontiers in Cellular and Infection Microbiology*, *7*(FEB). https://doi.org/10.3389/fcimb.2017.00039
2. Malhotra, S., Hayes, D. & Wozniak, D. J. Cystic Fibrosis and Pseudomonas aeruginosa: the Host-Microbe Interface. *Clin. Microbiol. Rev.* **32**, e00138-18 (2019).
3. Centers for Disease Control and Prevention. (2019). *Multidrug-resistant Pseudomonas aeruginosa* . Retrieved from https://www.cdc.gov/drugresistance/pdf/threats-report/pseudomonas-aeruginosa-508.pdf
4. Lee, K. & Yoon, S. S. Pseudomonas aeruginosa Biofilm, a Programmed Bacterial Life for Fitness. *J. Microbiol. Biotechnol.* **27**, 1053–1064 (2017).
5. Wolcott, R.; Dowd, S., The role of biofilms: Are we hitting the right target? *Plastic and Reconstructive Surgery* **2011,** *127*, 28-35.
6. Ma, L., Conover, M., Lu, H., Parsek, M. R., Bayles, K., & Wozniak, D. J. (2009). Assembly and development of the Pseudomonas aeruginosa biofilm matrix. *PLoS Pathogens*, *5*(3). https://doi.org/10.1371/journal.ppat.1000354
7. Kovach, K. *et al.* Evolutionary adaptations of biofilms infecting cystic fibrosis lungs promote mechanical toughness by adjusting polysaccharide production. *npj Biofilms Microbiomes* **3**, 0–1 (2017).
8. Zhang, R., Xia, A., Ni, L., Li, F., Jin, Z., Yang, S., & Jin, F. (2017). Strong Shear Flow Persister Bacteria Resist Mechanical Washings on the Surfaces of Various Polymer Materials. *Advanced Biosystems*, *1*(12), 1700161. https://doi.org/10.1002/adbi.201700161
9. Dominguez-Benetton, X. Biocomplexity and Bioelectrochemical Influence of Gasoline Pipelines Biofilms in Carbon Steel Deterioration: A Transmission Lines and Transfer Functions Approach. (2007).
10. Jensen, P. Ø., Givskov, M., Bjarnsholt, T. & Moser, C. The immune system vs. Pseudomonas aeruginosa biofilms. *FEMS Immunol. Med. Microbiol.* **59**, 292–305 (2010).
11. Walters III, M. C., Roe, F., Bugnicourt, A., Franklin, M. J., & Stewart, P. S. (2003). Contributions of Antibiotic Penetration, Oxygen Limitation. *Antimicrobial Agents and Chemotherapy*, *47*(1), 317–323. https://doi.org/10.1128/AAC.47.1.317
12. Wessel, A. K. *et al.* Oxygen Limitation within a Bacterial Aggregate. *MBio* **5**, e00992-14 (2014).

13. Ciofu, O., Rojo-Molinero, E., Macià, M. D., & Oliver, A. (2017). Antibiotic treatment of biofilm infections. *Apmis*, *125*(4), 304–319. https://doi.org/10.1111/apm.12673
14. Jensen, P. Ø., Givskov, M., Bjarnsholt, T. & Moser, C. The immune system vs. Pseudomonas aeruginosa biofilms. *FEMS Immunol. Med. Microbiol.* **59**, 292–305 (2010).
15. Kostakioti, M., Hadjifrangiskou, M., & Hultgren, S. J. (2013). Bacterial biofilms: Development, dispersal, and therapeutic strategies in the dawn of the postantibiotic era. *Cold Spring Harbor Perspectives in Medicine*, *3*(4), 1–23. https://doi.org/10.1101/cshperspect.a010306
16. Hall-Stoodley, L.; Costerton, J. W.; Stoodley, P., Bacterial biofilms: From the natural environment to infectious diseases. *Nature Reviews Microbiology* **2004,** *2*, 95-108.
17. Flemming, H. C.; Wingender, J.; Szewzyk, U.; Steinberg, P.; Rice, S. A.; Kjelleberg, S., Biofilms: An emergent form of bacterial life. *Nature Reviews Microbiology* **2016,** *14*, 563-575
18. Valentini, M.; Filloux, A., Biofilms and Cyclic di-GMP (c-di-GMP) signaling: Lessons from Pseudomonas aeruginosa and other bacteria. *Journal of Biological Chemistry* **2016,** *291*, 12547-12555.
19. Rodesney, C. A.; Roman, B.; Dhamani, N.; Cooley, B. J.; Katira, P.; Touhami, A.; Gordon, V. D., Mechanosensing of shear by Pseudomonas aeruginosa leads to increased levels of the cyclic-di-GMP signal initiating biofilm development. *Proceedings of the National Academy of Sciences of the USA* **2017,** *114* (23), 5906-5911.
20. Duvernoy, M. C., Mora, T., Ardré, M., Croquette, V., Bensimon, D., Quilliet, C., Desprat, N. (2018). Asymmetric adhesion of rod-shaped bacteria controls microcolony morphogenesis. *Nature Communications*, *9*(1), 25–28. https://doi.org/10.1038/s41467-018-03446-y
21. Bjarnsholt, T., Alhede, M., Alhede, M., Eickhardt-Sørensen, S. R., Moser, C., Kühl, M., … Høiby, N. (2013). The in vivo biofilm. *Trends in Microbiology*, *21*(9), 466–474. https://doi.org/10.1016/j.tim.2013.06.002
22. Stoodley, P., Sauer, K., Davies, D. G. & Costerton, J. W. Biofilms as Complex Differentiated Communities. *Annu. Rev. Microbiol.* **56**, 187–209 (2002).
23. Nadell, C. D.; Drescher, K.; Foster, K. R., Spatial structure, cooperation and competition in biofilms. *Nature Reviews Microbiology* **2016,** *14*, 589-600.
24. Tuson, H. H.; Weibel, D. B., Bacteria–surface interactions. *Soft Matter* **2013,** *9* (17), 4368-4380.
25. González, J. F.; Hahn, M. M.; Gunn, J. S., Chronic biofilm-based infections: skewing of the immune response. *Pathogens and Disease* **2018,** *76* (3)

26. Khatoon, Z.; McTiernan, C. D.; Suuronen, E. J.; Mah, T.-F.; Alarcon, E. I., Bacterial biofilm formation on implantable devices and approaches to its treatment and prevention. *Heliyon* **2018,** *4* (12).
27. Verderosa, A. D.; Totsika, M.; Fairfull-Smith, K. E., Bacterial Biofilm Eradication Agents: A Current Review. *Frontiers in Chemistry* **2019,** *7* (824).
28. Costerton, J. W.; Stewart, P. S.; Greenberg, E. P., Bacterial biofilms: A common cause of persistent infections. *Science* **1999,** *284*, 1318-1322.
29. James, G. A.; Swogger, E.; Wolcott, R.; Pulcini, E. D.; Secor, P.; Sestrich, J.; Costerton, J. W.; Stewart, P. S., Biofilms in chronic wounds. *Wound Repair and Regeneration* **2008,** *16*, 37-44.
30. Verma, A., Differences in Bacterial Colonization and Biofilm Formation Property of Uropathogens between the Two most Commonly used Indwelling Urinary Catheters. *Journal of Clinical and Diagnostic Research* **2016**, 1-3.
31. Deva, A. K.; Adams, W. P.; Vickery, K., The role of bacterial biofilms in device-associated infection. *Plastic and Reconstructive Surgery* **2013,** *132*, 1319-1328.
32. Veerachamy, S.; Yarlagadda, T.; Manivasagam, G.; Yarlagadda, P. K. D. V., Bacterial adherence and biofilm formation on medical implants: A review. *Proceedings of the Institution of Mechanical Engineers, Part H: Journal of Engineering in Medicine* **2014,** *228*, 1083-1099.
33. Ribeiro, M.; Monteiro, F. J.; Ferraz, M. P., Infection of orthopedic implants with emphasis on bacterial adhesion process and techniques used in studying bacterial-material interactions. *Biomatter* **2012,** *2* (4), 176-194.
34. Moriarty, F.; Zaat, S. A. J.; Busscher, H. J., *Biomaterials Associated Infection: Immunological aspects and antimicrobial strategies*. Springer: New York, 2013.
35. Gupta, K.; Liao, J.; Petrova, O.; Cherney, K. E.; Sauer, K., Elevated levels of the second messenger c-di-GMP contribute to antimicrobial resistance of Pseudomonas aeruginosa. *Mol Microbiol.* **2014,** *23*, 1-7.
36. Cotter, P. A.; Stibitz, S., c-di-GMP-mediated regulation of virulence and biofilm formation. *Current Opinion in Microbiology* **2007,** *10*, 17-23.
37. Hengge, R., Principles of c-di-GMP signalling in bacteria. *Nature Reviews Microbiology* **2009,** *7*, 263-273.
38. Luo, Y.; Zhao, K.; Baker, A.; Kuchma, S.; Coggan, K.; Wolfgang, M.; Wong, G.; O'Toole, G., A Hierarchical Cascade of Second Messengers Regulates Pseudomonas aeruginosa Surface Behaviors. *mBio* **2015,** *6* (1), e02456-14.
39. Song, F.; Wang, H.; Sauer, K.; Ren, D., Cyclic-di-GMP and oprF are involved in the response of Pseudomonas aeruginosa to substrate material stiffness during attachment on polydimethylsiloxane (PDMS). *Frontiers in Microbiology* **2018,** *9*, 1-13.

40. Kolewe, K.; Zhu, J.; Mako, N.; Nonnenmann, S.; Schiffman, J., Bacterial Adhesion Is Affected by the Thickness and Stiffness of Poly(ethylene glycol) Hydrogels. *ACS Applied Materials and Interfaces* **2018,** *10*, 2275-2281.
41. Janmey, P. A.; Fletcher, D. A.; Reinhart-King, C. A., Stiffness Sensing by Cells. *Physiological Reviews* **2020,** *100* (2), 695-724.
42. Feng, J.; Levine, H.; Mao, X.; Sander, L. M., Cell motility, contact guidance, and durotaxis. *Soft Matter* **2019,** *15* (24), 4856-4864.
43. Jiang, L.; Sun, Z.; Chen, X.; Li, J.; Xu, Y.; Zu, Y.; Hu, J.; Han, D.; Yang, C., Cells Sensing Mechanical Cues: Stiffness Influences the Lifetime of Cell–Extracellular Matrix Interactions by Affecting the Loading Rate. *ACS Nano* **2016,** *10* (1), 207-217.
44. Jaalouk, D. E.; Lammerding, J., Mechanotransduction gone awry. *Nature Reviews Molecular Cell Biology* **2009,** *10*, 63-73.
45. Iskratsch, T.; Wolfenson, H.; Sheetz, M. P., Appreciating force and shape-the rise of mechanotransduction in cell biology. *Nature Reviews Molecular Cell Biology* **2014,** *15*, 825-833.
46. Wang, N., Review of cellular mechanotransduction. *Journal of Physics D: Applied Physics* **2017,** *50*.
47. Imani, S. M.; Maclachlan, R.; Rachwalski, K.; Chan, Y.; Lee, B.; McInnes, M.; Grandfield, K.; Brown, E. D.; Didar, T. F.; Soleymani, L., Flexible Hierarchical Wraps Repel Drug-Resistant Gram-Negative and Positive Bacteria. *ACS Nano* **2020,** *14* (1), 454-465.
48. Feng, G.; Cheng, Y.; Wang, S.-Y.; Borca-Tasciuc, D. A.; Worobo, R. W.; Moraru, C. I., Bacterial attachment and biofilm formation on surfaces are reduced by small-diameter nanoscale pores: how small is small enough? *npj Biofilms and Microbiomes* **2015,** *1* (1), 15022.
49. Mann, B. K.; Gobin, A. S.; Tsai, A. T.; Schmedlen, R. H.; West, J. L., Smooth muscle cell growth in photopolymerized hydrogels with cell adhesive and proteolytically degradable domains: Synthetic ECM analogs for tissue engineering. *Biomaterials* **2001,** *22*, 3045-3051.
50. Bryant, S. J.; Anseth, K. S., Controlling the spatial distribution of ECM components in degradable PEG hydrogels for tissue engineering cartilage. **2002**.
51. Stosich, M. S.; Mao, J. J., Adipose tissue engineering from human adult stem cells: Clinical implications in plastic and reconstructive surgery. *Plastic and Reconstructive Surgery* **2007,** *119*, 71-83.
52. Nachlas, A. L. Y.; Li, S.; Jha, R.; Singh, M.; Xu, C.; Davis, M. E., Human iPSC-derived mesenchymal stem cells encapsulated in PEGDA hydrogels mature into valve interstitial-like cells. *Acta Biomaterialia* **2018,** *71*, 235-246.
53. Zhai, X.; Ruan, C.; Ma, Y.; Cheng, D.; Wu, M.; Liu, W.; Zhao, X.; Pan, H.; Lu, W. W., 3D-Bioprinted Osteoblast-Laden Nanocomposite Hydrogel Constructs

with Induced Microenvironments Promote Cell Viability, Differentiation, and Osteogenesis both In Vitro and In Vivo. *Advanced Science* **2018,** *5* (3), 1700550.
54. Lim, W. S.; Chen, K.; Chong, T. W.; Xiong, G. M.; Birch, W. R.; Pan, J.; Lee, B. H.; Er, P. S.; Salvekar, A. V.; Venkatraman, S. S.; Huang, Y., A bilayer swellable drug-eluting ureteric stent: Localized drug delivery to treat urothelial diseases. *Biomaterials* **2018,** *165*, 25-38.
55. Choi, J. R.; Yong, K. W.; Choi, J. Y.; Cowie, A. C., Recent advances in photo-crosslinkable hydrogels for biomedical applications. *BioTechniques* **2019,** *66* (1), 40-53.
56. Browning, M. B.; Wilems, T.; Hahn, M.; Cosgriff-Hernandez, E., Compositional control of poly(ethylene glycol) hydrogel modulus independent of mesh size. *Journal of Biomedical Materials Research Part A* **2011,** *98A* (2), 268-273.
57. Navarro, A. P., Collins, M. A., & Folker, E. S. (2016). The nucleus is a conserved mechanosensation and mechanoresponse organelle. *Cytoskeleton*, *73*(2), 59–67. https://doi.org/10.1002/cm.21277
58. Jan, N., Jin, P., Jan, L. Y. & Jan, Y. Mechanosensitive Ion Channels: Structural Features Relevant to Mechanotransduction Mechanisms. *Trends Pharmacol. Sci.* **8**, 236 (1987).
59. Gordon, V. D. & Wang, L. Bacterial mechanosensing: the force will be with you, always. *J. Cell Sci.* **132**, jcs227694 (2019).
60. Merz, A. J., So, M. & Sheetz, M. P. Pilus retraction powers bacterial twitching motility. *Nature* **407**, 98–102 (2000).
61. Siryaporn, A.; Kuchma, S.; O'Toole, G.; Gitai, Z., Surface attachment induces Pseudomonas aeruginosa virulence. *Proceedings of the National Academy of Sciences of the USA* **2014,** *111* (47), 16860-16865.
62. Otto, K. & Silhavy, T. J. Surface sensing and adhesion of Escherichia coli controlled by the Cpx-signaling pathway. *Proc. Natl. Acad. Sci. U. S. A.* **99**, 2287–2292 (2002).
63. Jacobs, M. A.; Alwood, A.; Thaipisuttikul, I.; Spencer, D.; Haugen, E.; Ernst, S.; Will, O.; Kaul, R.; Raymond, C.; Levy, R.; Chun-Rong, L.; Guenthner, D.; Bovee, D.; Olson, M. V.; Manoil, C., Comprehensive transposon mutant library of Pseudomonas aeruginosa. *Proceedings of the National Academy of Sciences* **2003,** *100* (24), 14339-14344.
64. Rybtke, M. T.; Borlee, B. R.; Murakami, K.; Irie, Y.; Hentzer, M.; Nielsen, T. E.; Givskov, M.; Parsek, M. R.; Tolker-Nielsen, T., Fluorescence-based reporter for gauging cyclic Di-GMP levels in Pseudomonas aeruginosa. *Applied and Environmental Microbiology* **2012,** *78*, 5060-5069.
65. Hahn, M. S.; Taite, L. J.; Moon, J. J.; Rowland, M. C.; Ruffino, K. A.; West, J. L., Photolithographic patterning of polyethylene glycol hydrogels. *Biomaterials* **2006,** *27*, 2519-2524.

66. Schindelin, J.; Arganda-Carreras, I.; Frise, E.; Kaynig, V.; Longair, M.; Pietzsch, T.; Preibisch, S.; Rueden, C.; Sallfeld, S.; Schmid, B.; Tinevez, J.-Y.; James White, D.; Hartenstein, V.; Eliceiri, K.; Tomancak, P.; Cardona, A., Fiji: an open-source platform for biological-image analysis. *Nature Methods* **2012,** *9*, 676-682.
67. Stephens, M. A., EDF Statistics for Goodness of Fit and Some Comparisons. *Journal of the American Statistical Association* **1974,** *69* (347), 730-737.
68. Armbruster, C. R.; Lee, C. K.; Parker-Gilham, J.; de Anda, J.; Xia, A.; Tseng, B. S.; Hoffman, L. R.; Jin, F.; Harwood, C. S.; Wong, G. C. L.; Parsek, M. R., Heterogeneity in surface sensing produces a division of labor in Pseudomonas aeruginosa populations. **2019**.
69. Westfall, P. H., Kurtosis as Peakedness, 1905 - 2014. R.I.P. *Am Stat* **2014,** *68* (3), 191-195.
70. Orans, J.; Johnson, M. D. L.; Coggan, K. A.; Sperlazza, J. R.; Heiniger, R. W.; Wolfgang, M. C.; Redinbo, M. R., Crystal structure analysis reveals Pseudomonas PilY1 as an essential calcium-dependent regulator of bacterial surface motility. *Proceedings of the National Academy of Sciences of the United States of America* **2010,** *107*, 1065-1070.
71. Kuchma, S. L.; Ballok, A. E.; Merritt, J. H.; Hammond, J. H.; Lu, W.; Rabinowitz, J. D.; O'Toole, G. A., Cyclic-di-GMP-mediated repression of swarming motility by Pseudomonas aeruginosa: The pilY1 gene and its impact on surface-associated behaviors. *Journal of Bacteriology* **2010,** *192*, 2950-2964.
72. Chuang, S. K.; Vrla, G. D.; Fröhlich, K. S.; Gitai, Z., Surface association sensitizes Pseudomonas aeruginosa to quorum sensing. *Nature Communications* **2019,** *10* (1), 4118.
73. Sanfilippo, J. E.; Lorestani, A.; Koch, M. D.; Bratton, B. P.; Siryaporn, A.; Stone, H. A.; Gitai, Z., Microfluidic-based transcriptomics reveal force-independent bacterial rheosensing. *Nature Microbiology* **2019,** *4* (8), 1274-1281.
74. Baker, A. E.; Webster, S. S.; Diepold, A.; Kuchma, S. L.; Bordeleau, E.; Armitage, J. P.; O'Toole, G. A., Flagellar Stators Stimulate c-di-GMP Production by Pseudomonas aeruginosa. *Journal of Bacteriology* **2019,** *201* (18), e00741-18.
75. Schniederberend, M.; Williams, J. F.; Shine, E.; Shen, C.; Jain, R.; Emonet, T.; Kazmierczak, B. I., Modulation of flagellar rotation in surface-attached bacteria: A pathway for rapid surface-sensing after flagellar attachment. *PLOS Pathogens* **2019,** *15* (11), e1008149.
76. Whittaker, C. & Hynes, R. O. Distribution and Evolution of von Willebrand/Integrin A Domains: Widely Dispersed Domains with Roles in Cell Adhesion and Elsewhere. *Mol. Biol. Cell* **13**, 4100–4109 (2002).